A&A 454, 503–509 (2006)
DOI: 10.1051/0004-6361:20065226
© ESO 2006

Astronomy & Astrophysics

Supernova 2006aj and the associated X-Ray Flash 060218⋆,⋆⋆

J. Sollerman[1,2], A. O. Jaunsen[3], J. P. U. Fynbo[1], J. Hjorth[1], P. Jakobsson[1], M. Stritzinger[1], C. Féron[1], P. Laursen[1], J.-E. Ovaldsen[3], J. Selj[3], C. C. Thöne[1], D. Xu[1], T. Davis[1], J. Gorosabel[4], D. Watson[1], R. Duro[3], I. Ilyin[5], B. L. Jensen[1], N. Lysfjord[3], T. Marquart[6], T. B. Nielsen[7], J. Näränen[8], H. E. Schwarz[9], S. Walch[10], M. Wold[11], and G. Östlin[2]

[1] Dark Cosmology Centre, Niels Bohr Institute, University of Copenhagen, Juliane Maries Vej 30, 2100 Copenhagen Ø, Denmark
[2] Stockholm Observatory, Department of Astronomy, AlbaNova, 106 91 Stockholm, Sweden
[3] Institute of Theoretical Astrophysics, PO Box 1029, 0315 Oslo, Norway
[4] Instituto de Astrofisica de Andalucia (IAA-CSIC), PO Box 03004, 18080 Granada, Spain
[5] Astrophysikalisches Institut, An der Sternwarte 16, 14482 Potsdam, Germany
[6] Dept. of Astronomy and Space Physics, Box 515, 751 20 Uppsala, Sweden
[7] NOT, Apartado 474, 38700 Santa Cruz de la Palma, Spain
[8] Observatory, University of Helsinki, PO Box 14, 00014, Finland
[9] CTIO-NOAO, Casilla 603, La Serena, Chile
[10] University Observatory Munich, Scheinerstr. 1, 81679 Munich, Germany
[11] ESO, Karl-Schwarzschild-Strasse 2, 85748 Garching, Germany

Received 17 March 2006 / Accepted 15 April 2006

ABSTRACT

Aims. We have studied the afterglow of the gamma-ray burst (GRB) of February 18, 2006. This is a nearby long GRB, with a very low peak energy, and is therefore classified as an X-ray Flash (XRF). XRF 060218 is clearly associated with a supernova – dubbed SN 2006aj.
Methods. We present early spectra for SN 2006aj as well as optical lightcurves reaching out to 50 days past explosion.
Results. Our optical lightcurves define the rise times, the lightcurve shapes and the absolute magnitudes in the U, V and R bands, and we compare these data with data for other relevant supernovae. SN 2006aj evolved quite fast, somewhat similarly to SN 2002ap, but not as fast as SN 1994I. Our spectra show the evolution of the supernova over the peak, when the U-band portion of the spectrum rapidly fades due to extensive line blanketing. We compare to similar spectra of very energetic type Ic supernovae. Our first spectra are earlier than spectra for any other GRB-SN. The spectrum taken 12 days after burst in the rest frame is similar to somewhat later spectra of both SN 1998bw and SN 2003dh, implying a rapid early evolution. This is consistent with the fast lightcurve.
From the narrow emission lines from the host galaxy we derive a redshift of $z = 0.0331 \pm 0.0007$. This makes XRF 060218 the second closest gamma-ray burst detected. The flux of these emission lines indicate a high-excitation state, and a modest metallicity and star formation rate of the host galaxy.

Key words. gamma rays: bursts – supernovae: individual: SN 2006aj

1. Introduction

The last few years have settled the debate about the origin of long gamma-ray bursts (GRBs). The hint provided by GRB 980425 and SN 1998bw (Galama et al. 1998) was finally taken when the spectroscopic follow-up of the afterglow of GRB 030329 revealed the unambiguous signatures of a very energetic supernova – SN 2003dh (Hjorth et al. 2003; Matheson et al. 2003; Stanek et al. 2003). Soon thereafter, another clear-cut SN 1998bw look-alike emerged in the afterglow of GRB 031203 (Malesani et al. 2004; Thomsen et al. 2004). While the Swift satellite (Gehrels et al. 2004) has been very successful in finding GRBs over a large redshift range (e.g., Jakobsson et al. 2006), the wait for the next spectacular case of a nearby GRB-supernova has lasted more than two years.

1.1. GRB 060218

GRB 060218 was detected by the BAT instrument on-board the Swift satellite (Cusumano et al. 2006) on February 18.149 2006 UT. This burst had exceptional high-energy properties (Campana et al. 2006). The peak energy of the event (Sect 4.2.3) was very low and we will hereafter refer to this burst as an X-ray flash. XRF 060218 is one of the longest bursts ever detected, and the unusual properties gave a very confused early impression. Several GCNs indicated that this was probably not a proper GRB, and our optical monitoring programme was therefore somewhat delayed. However, eventually this turned out to be a very interesting low-z event (Mirabal et al. 2006) with a likely association to a supernova (Masetti et al. 2006; Soderberg et al. 2006b). The transient has now been detected over a wide wavelength range, from X-rays (Kennea et al. 2006) to radio (Soderberg et al. 2006a).

⋆ This paper is based on observations from the ESO/Danish 1.5-m telescope at the La Silla Observatory and on observations made with the Nordic Optical Telescope, operated on the island of La Palma jointly by Denmark, Finland, Iceland, Norway, and Sweden, in the Spanish Observatorio del Roque de los Muchachos of the Instituto de Astrofisica de Canarias.

⋆⋆ Table 1 is only available in electronic form at `http://www.edpsciences.org`

Article published by EDP Sciences and available at http://www.edpsciences.org/aa or http://dx.doi.org/10.1051/0004-6361:20065226

In this paper we focus on the optical transient, and the early spectral and photometric evolution of this supernova (SN). The paper is organized as follows. Section 2 outlines how the optical observations were obtained and reduced. The results are presented in Sect. 3, which includes U-, V- and R-band lightcurves as well as spectra of the SN, and an analysis of the host galaxy. We end the paper with a discussion (Sect. 4) where we compare the properties of this SN with other relevant SNe.

2. Observations

2.1. Photometry

The observations for XRF 060218 were somewhat complicated and hampered by the celestial position of the burst. Being close to the Sun it could only be observed for a short time right after sunset. We have used the combined efforts of two telescopes, at a northern and a southern observatory, to follow the object until it faded into the glare of the Sun, about 50 days past the burst. For the final observations we had to restrict ourselves to a single passband (R) due to the limited time available for observations in the twillight.

We obtained imaging of the transient of XRF 060218 with the ESO/Danish 1.5 m telescope (D1.5 m) on La Silla equipped with the DFOSC instrument, which offers a 13.7×13.7 arcmin field-of-view (FOV) at 0.395 arcsec per pixel. We also used the 2.56 m Nordic Optical Telescope (NOT) on La Palma equipped with ALFOSC which offers a FOV of 6.3×6.3 arcmin with a pixel scale of 0.189 arcsec, as well as StanCam which has a pixel scale of 0.176 arcsec over 3×3 arcmin.

The journal of observations is given in Table 4. The data were reduced using standard techniques for de-biasing and flat-fielding.

2.2. Spectroscopy

Spectra of the source were obtained with ALFOSC at four epochs, February 21, 22 and 24 and on March 2. These epochs correspond to 3.78, 4.71, 6.71 and 12.71 days past the burst. Each spectrum had an integration time of 2400 s using grism 4 and a 1.3 arcsec wide slit. This set-up provided a dispersion of 3 Å per pixel. The spectral range covered is from 3300 to 9200 Å. There is some second order contamination above 6600 Å, and significant fringing above ~7500 Å. The spectra were taken at or close to the parallactic angle. We note that apart from the first spectrum, taken at an airmass of 1.93, all spectra were achieved at an airmass <1.5. The NOT/ALFOSC has a high efficiency in the UV, so we put emphasis on obtaining the bluest part of the spectrum.

The spectra were reduced following standard procedures in `MIDAS` and `IRAF`. Wavelength calibration was achieved by comparison to images taken of helium and neon lamps. The flux calibration was performed using the spectrophotometric standard star GD71 (Bohlin et al. 1995), which was observed every night close in time to the supernova observation. Finally, the absolute flux-calibration was achieved by comparison to the contemporary (or interpolated) V-band photometry.

When comparing to synthetic photometry obtained by integrating each spectrum under the filter profiles, we discovered that some of the spectra have suffered from differential slit losses. This has been considered in the analysis below.

3. Results

3.1. The lightcurves

Aperture photometry of the transient was carried out using a combination of `DAOPHOT` (Stetson 1987) and `SExtractor` (Bertin & Arnouts 1996). We measured the magnitudes of the supernova as well as for 9 stars in the field in the V and R bands (7 local standards in the U band). The relative magnitudes were transformed to the standard system using observations of photometric standard stars (Landolt 1992). We estimate an absolute photometric accuracy of 0.08, 0.06 and 0.04 mag in the U, V and R bands, respectively.

In Fig. 1 we plot the U-, V- and R-band lightcurves. This is the data from Table 4. The dates are given with respect to the time of the burst in the observers frame. We have not plotted the data with errors larger than 0.15 mag, if there are more accurate data from the same night. The R- and V-band lightcurves are followed from well before peak and are traced to way past maximum.

In Fig. 1 we have applied no corrections to subtract the host galaxy (estimated at $R = 19.9$, see Sect. 3.3). This can be an important contribution, ~0.1 mag at maximum light, and is considered in the following analysis. Also, we have made no K-corrections for the magnitudes given in Table 4 and plotted in Fig. 1. At the early epochs where we have spectra, we estimate this correction to be ~0.04 mag in the V band, and 0.11 mag in the R band. The final spectrum is taken closest in time to the maximum light in these bands, and indicate K-corrections of ~0.02 mag in the V band, and 0.15 mag in R.

To estimate the time of maximum, peak brightness and the lightcurve shape as described by Δm_{15} (the number of magnitudes the supernova decayed in the 15 days following maximum brightness) we have fitted the lightcurves with smooth functions (see Stritzinger et al. 2006). We estimate the rise times of $t(V) = 10.4 \pm 0.5$ days past burst and $t(R) = 11.4 \pm 0.5$ days. We further estimate $\Delta m_{15}(V) = 0.92$ and $\Delta m_{15}(R) = 0.71$ mag from the observed data. When correcting for the underlying emission from the host galaxy (Sect. 3.3.2), as well as for time dilation, the corrected numbers are $\Delta m_{15}(V) = 1.1 \pm 0.1$ and $\Delta m_{15}(R) = 0.90 \pm 0.1$ mag.

The peak magnitudes are estimated to be $m(V) = 17.47 \pm 0.05$ and $m(R) = 17.22 \pm 0.05$ mag. To determine the absolute magnitudes we need estimates of the distance and extinction. The redshift of this burst is $z = 0.0331$ (Mirabal et al. 2006, see also Sect. 3.2), and assuming a cosmology where $H_0 = 70\,\mathrm{km\,s^{-1}\,Mpc^{-1}}$, $\Omega_\Lambda = 0.7$ and $\Omega_\mathrm{m} = 0.3$, this corresponds to a luminosity distance of 145.4 Mpc.

The reddening associated with Galactic extinction is $E(B-V) = 0.14$ mag according to the maps by Schlegel et al. (1998). High-resolution spectra (Guenther et al. 2006) can be used to check this. Using the sodium lines to estimate the reddening (see e.g., Munari & Zwitter 1997) provides $E(B-V) = 0.127$ for the Milky Way, and $E(B-V) = 0.042$ mag for the GRB host. This is consistent with adopting a total reddening of $E(B-V) = 0.14$ mag. We note that Campana et al. (2006) required $E(B-V)_\mathrm{host} = 0.20$ mag based on the assumption of thermal radiation detected by UVOT. This is higher than claimed by Guenther et al. (2006). It is known that the Na I D lines do not provide a robust measure of the extinction, and could be influenced by e.g., the ionization state in the host (see e.g., Sollerman et al. 2005a,b). However, the overall properties of the host galaxy based on the spectral energy distribution (SED) modeling (Sect. 3.3.1), as well as the measured Balmer line decrement (Sect. 3.3.2, see also Pian et al. 2006), also argue for

Table 2. Strong emission lines.

ID	Rest wavelength (Å)	Observed wavelength (Å)	Flux (10^{-16} erg s^{-1} cm^{-2})	Redshift
[O II]	3727.42	3853.42	16	0.0338
Hβ	4861.33	5021.00	11	0.0328
[O III]	4958.91	5121.76	16	0.0328
[O III]	5006.84	5171.18	46	0.0328
Hα	6563.00	6778.14	20	0.0328

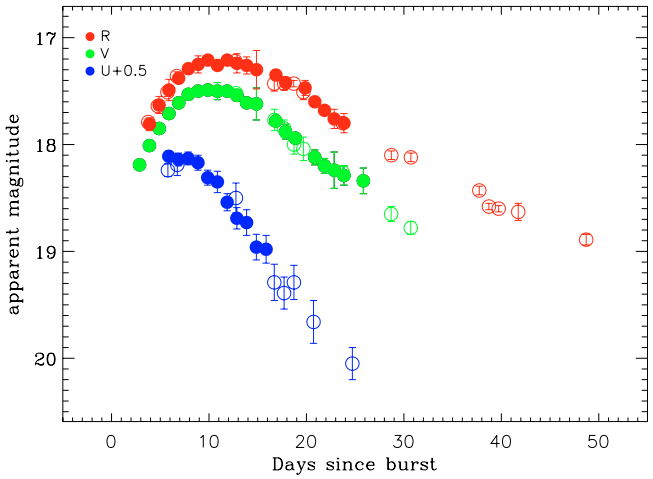

Fig. 1. The U-, V- and R-band lightcurves of SN 2006aj. Dates are given in days after the high-energy burst in the observers frame. The filled circles are data from the D1.5 m, and the open circles from the NOT (data from Table 4). For clarity, we have excluded points for which the errors are greater than 0.15 mag when more accurate data were available for the same night. These magnitudes are not corrected for the host galaxy contribution, and have not been K-corrected. Corrections for the host galaxy is done in Fig. 5.

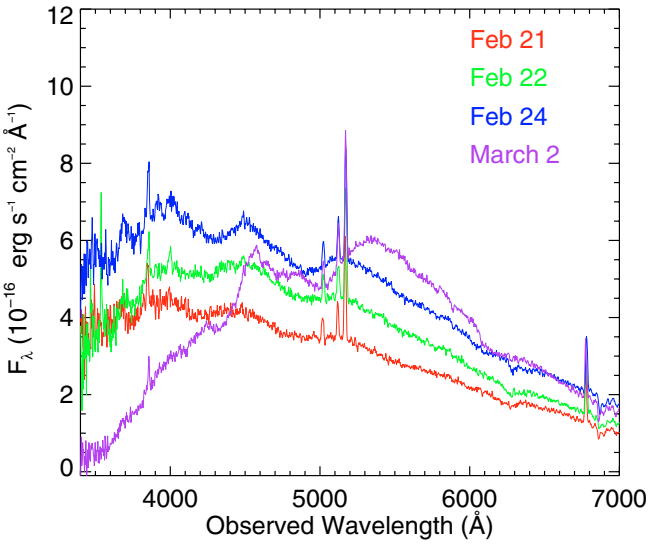

Fig. 2. The flux-calibrated and de-reddened spectra of the emerging supernova. The spectra have been absolute flux-calibrated by comparison to V-band photometry. In the Feb. 24 spectrum we note some components of intermediate widths ~3000−4000 km s^{-1} in the blue part of the spectrum.

a low host extinction. In the following we will therefore adopt a total extinction of $E(B-V) = 0.14$ mag.

The absolute magnitudes of the SN are then $M(V) = -18.8$ and $M(R) = -18.9$ mag. Finally, correcting these estimates for host contamination ($V, R = 0.09, 0.10$) and K-corrections ($V, R = 0.02, 0.15$) our best estimates are $M(V) = -18.7$ and $M(R) = -18.7$ mag. These are the magnitudes adopted for comparison to other SNe, and are given in Table 3.

3.1.1. The *U*-band lightcurve

Lightcurves for type Ic SNe are relatively rare in the U band. For SN 2006aj, we started our U-band imaging campaign 5 days past the burst. At this epoch, the U band was already close to maximum light. We then followed the evolution of the U-band flux until 25 days past the burst, after which the supernova became to faint (also compared to the host) to allow further monitoring.

Given the sparse pre-maximum coverage, the estimates are somewhat more uncertain in the U band. We estimate $t(U) = 6.8 \pm 1.0$ days. The estimate of the corrected light curve shape is rather uncertain, due to the large correction for host contamination on the already steep lightcurve. We estimate $\Delta m_{15}(U) = 2.0 \pm 0.2$. The peak brightness is $m(U) = 17.60 \pm 0.10$ mag, which converts to an absolute U-band magnitude of $M(U) = -18.9$ in the Vega magnitude system.

The K-corrections are most uncertain in the U band, and could also be significant in particular for the latest epochs where the spectrum falls very steeply in that region. At around U-band maximum light, we estimate a K-correction of ~−0.15 mag. Applying this K-correction, and a correction for the host galaxy (0.08 mag) we therefore estimate the final absolute magnitude $M(U) = -18.9$.

We summarize all corrected lightcurve parameters in Table 3. In this table, the rise times are corrected for time dilation, as are the light curve shapes which are also corrected for the underlying host galaxy. The absolute magnitudes are corrected for extinction, host galaxy contamination and are K-corrected.

3.2. The spectral evolution

The flux-calibrated spectra are shown in Fig. 2. The continuum-like spectrum with broad bumps renders a classification of this burst as a type Ic supernova, based on the lack of conspicuous SN lines (e.g., Patat et al. 2001).

The spectral evolution is well represented, the most obvious development being the depression of the UV flux with time. Some of the depression seen in our final spectrum may be attributed to differential slit losses, but the overall evolution of the spectra are correct, as can be seen from the comparison to the broad band light curves. In fact, the UV depression is a common feature of SNe and reflects the increased line blanketing due to low ionization iron group elements. As seen from the lightcurve, the U band actually peaked close to the date of our third spectrum, so we see the rise of the U band up to that epoch

Table 3. Final corrected light curve estimates.

	U	V	R
Rise time (days)	6.6	10.0	11.0
Δm_{15} (mag)	2.0	1.1	0.90
Abs. Mag	−18.95	−18.65	−18.68

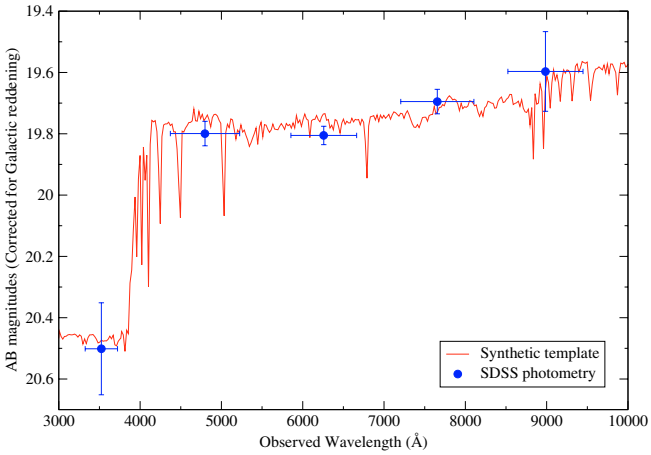

Fig. 3. The *ugriz*-band SED of the XRF 060218 host galaxy. The fit shows the best SED fit achieved (χ^2/d.o.f. = 1.38) when a SMC-like extinction law is assumed. This gives $A_V = 0.0$ mag.

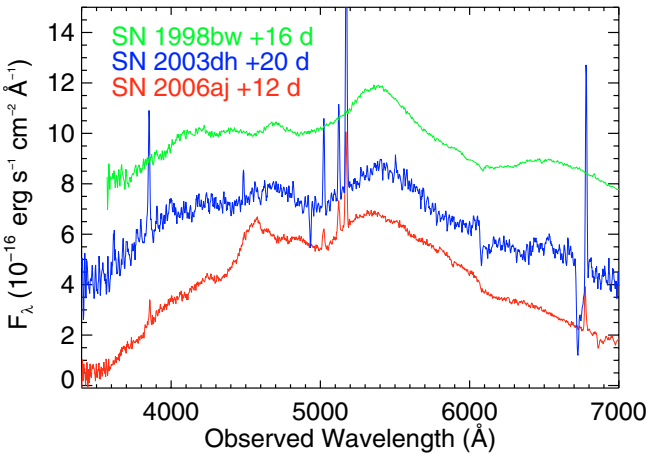

Fig. 4. Spectral comparison to other GRB SNe, SN 1998bw at 16 days past burst and SN 2003dh at 20 days past burst. Times are in the SN rest frames. The spectra of SNe 1998bw and 2003dh have been arbitrarily shifted in flux. They have also been shifted to the redshift of SN 2006aj. Note that SN 2003dh has an afterglow that adds to the UV part.

in the spectral evolution, followed by a rapid decline to the final spectrum.

Our latest spectrum, taken 12.3 days past burst in the rest frame, shows a dramatic evolution of the flux towards the red part of the spectrum. The broad red bumps are common features of so-called hypernovae and signal huge expansion velocities of the ejecta. Interpreting the inflection point at ∼6080 Å as the Si II 6355 Å feature seen in other GRB-SNe (Patat et al. 2001; Hjorth et al. 2003), we can estimate an expansion velocity of ∼22 000 km s^{-1}. At 12 days past burst, this is similar to the expansion velocities measured in SN 1998bw and SN 2003dh. However, since this feature is quite loosely defined, this estimate can only be approximate.

From the multitude of narrow emission lines from the host galaxy we can also measure the redshift to the supernova. The positions and fluxes of a number of detected narrow lines are given in Table 2. We derived the redshift by measuring the positions of the [O II] line, the [O III] lines as well as Hα and Hβ at all 4 epochs, and conclude $z = 0.0331 \pm 0.0007$.

The fluxes of the lines were measured by Gaussian fits, using both `IDL` and `IRAF splot`. We use these below to estimate the star formation rate and the metallicity. We note that the values given in Table 2 are averages for the four spectra corrected for $E(B-V) = 0.14$ mag. Apart from the stronger lines listed in Table 2, we also detect [Ne III] λ3869, which signals the presence of ionizing radiation. This line is about 3 times weaker than Hβ, although the uncertainty in such a weak line is ∼50% in our spectra. The stronger lines have uncertainties of $\lesssim$20%.

3.3. The host galaxy

3.3.1. Modeling the SED

The *ugriz*-band SDSS pre-imaging of the field (Cool et al. 2006) allowed us to construct the optical spectral energy distribution of the host galaxy. However, it was noted (Hicken et al. 2006; Modjaz et al. 2006) that the absolute calibration of this field was not correct. To correct the SDSS model magnitudes we used field star photometry (Hicken et al. 2006), which was transformed from Landolt to the SDSS-system using Jester et al. (2005). Corrected host magnitudes were then deduced from the offsets between the SDSS model magnitudes and the transformed values, giving: $u = 21.24 \pm 0.15, g = 20.29 \pm 0.04, r = 20.16 \pm 0.03, i = 19.96 \pm 0.04, z = 19.80 \pm 0.13$. We then used the best fit SED (see below) to transform these magnitudes back to Landolt photometry: $U = 20.45 \pm 0.15, B = 20.46 \pm 0.07, V = 20.19 \pm 0.04, R = 19.86 \pm 0.03, I = 19.47 \pm 0.06$ mag. These are the host galaxy magnitudes used to correct the light curve parameters in Sect. 3.1.

The *ugriz* host galaxy photometric points were then dereddened by the Galactic extinction following Schlegel et al. (1998) and then fitted based on the SDSS filter+CCD efficiency curves (Fukugita et al. 1996) and using the synthetic SED templates constructed with the HyperZ code (Bolzonella et al. 2000).

For the construction of the synthetic templates three initial mass functions (IMFs) were used (Scalo 1986; Miller & Scalo 1979; Salpeter 1955). We also used four different extinction laws: MW (Seaton 1979), LMC (Fitzpatrick 1986), SMC (Prevot et al. 1984) and one for starburst galaxies (Calzetti et al. 2000). Solar metallicity was assumed for all the templates. The redshift of the templates was fixed at $z = 0.0331$. In addition, a wide range of star-formation histories were considered (see more details on the τ parameter in Gorosabel et al. 2005), creating different families of templates: Elliptical, Starburst, Lenticular, Irregular and Spiral galaxies.

The *ugriz*-band photometric points were satisfactorily fitted by the SED templates ($\chi^2_{\rm d.o.f.} \sim 1.3$; see Fig. 3). Our SED fits did not favour any IMF, extinction law or galaxy type. This means that the inferred host galaxy extinction is independent on the input model, and is stable at around $A_V = 0.1$–0.3 mag. This is why we were favoring a low host galaxy extinction in Sect. 3.1.

3.3.2. Host galaxy properties

The host magnitude of $B = 20.46$ mag, and the Galactic extinction of $E(B-V) = 0.14$ gives an absolute magnitude for the

host of $M(B) = -15.9$ mag at the measured redshift. Adopting $M^B_\star = -21.1$ this corresponds to $L = 0.008 L^B_\star$.

From the Hα and [O II] lines we can estimate the star formation rate (SFR). From both these lines we get $SFR \sim 0.05\ M_\odot\ \mathrm{yr}^{-1}$, following Kennicutt (1998). This is of course only measured from the part of the galaxy that falls on the spectroscopic slit. The specific star formation rate for the host galaxy of XRF 060218 is thus $\sim 6\ M_\odot\ \mathrm{yr}^{-1}(L/L^\star)^{-1}$.

Finally, we can estimate the metallicity of the galaxy using the R23 technique. From the results presented in Table 2, we derive a $\log(R_{23}) = 0.8-0.9$. This indicates a somewhat subsolar metallicity, although the exact value can not be determined from this ratio alone (see e.g., Fig. 5 by Kewley & Dopita 2002).

The luminosity and star formation rate thus indicates a small but fairly normal dwarf galaxy, similar to other nearby GRB host galaxies (Sollerman et al. 2005b). The low metallicity is also similar to that of other GRB host galaxies.

4. Discussion

4.1. The supernova spectral evolution

The spectral evolution reveals a rapidly evolving type Ic supernova with very broad lines. Very few type Ic spectra exist for such early epochs. Our first spectrum was obtained 3.7 days past the burst. The first spectrum for SN 1998bw was not obtained until after a week, and for SN 2003dh the emission was still dominated by the afterglow at this epoch. Therefore, it is difficult to make any one-to-one comparisons of the apparent bumps in these spectra with those of other similar SNe (see e.g., Fig. 1 in Mazzali et al. 2002).

In Fig. 4 we have re-plotted our latest spectrum of SN 2006aj from March 2. This is 12.3 days past burst in the SN rest frame. We have also plotted spectra for SN 1998bw (Patat et al. 2001) and SN 2003dh (Hjorth et al. 2003). These spectra are very similar to the one for SN 2006aj, but are taken at a later epoch. SN 2006aj thus displays a fast spectral evolution. This agrees with the narrow lightcurve.

4.2. The supernova lightcurves

From the lightcurves, as well as from the spectral evolution, we can see that the emission is dominated by the supernova rather than by the afterglow from very early on. This is similar to SN 1998bw, where no optical afterglow was ever detected, but very different from SN 2003dh which was dominated by the afterglow for more than a week before it emerged.

4.2.1. The peak magnitude

The peak magnitudes we have estimated show that SN 2006aj was a fairly normal type Ic supernova in that respect (Richardson et al. 2006). In particular, it was not as bright as SN 1998bw or SN 2003dh. SN 1998bw ejected $0.35-0.50\ M_\odot$ of radioactive ^{56}Ni (see e.g., Sollerman et al. 2000; Woosley et al. 1999). That SN 2006aj was only $\sim$50% as luminous as SN 1998bw thus means that SN 2006aj ejected $\sim 0.22 \pm 0.06\ M_\odot$ of radioactive ^{56}Ni. This is still more than seen in other broad-line supernovae, such as SNe 1997ef and 2002ap. We note that the assumption that the peak magnitude scales with the nickel mass may not be valid for very asymmetric explosions (Hoeflich et al. 1999). GRBs are expected to be asymmetric, although they should all be pointed within a few degrees to our line of sight.

4.2.2. The light curve shape

The shape of the lightcurve is also of interest. For SN 2006aj we have summarized the properties in Table 3. For comparison, the type Ic SN 1994I displayed $\Delta m_{15}(U) \sim 2.5$ and $\Delta m_{15}(V) \sim 1.7$ mag. The peak magnitude for SN 1994I was reached after $\sim$8 days in U, and after 10 days in the V band (Richmond et al. 1996). The rise time is, however, very uncertain for SN 1994I; since the exact epoch of the explosion was not observed.

For SN 1998bw, Fynbo et al. (2004) estimated $\Delta m_{15}(U) \sim 1.3$ and $\Delta m_{15}(V) \sim 0.7$ mag. The peak magnitude was reached after 13.5 days in U, and after 17 days in the V band (Galama et al. 1998). This is clearly slower than observed for SN 2006aj. Finally, SN 2002ap reached U-band maximum at about 6.2 days (Foley et al. 2003; Gal-Yam et al. 2002; Pandey et al. 2003). This lightcurve seems to be most similar to SN 2006aj in this respect. In Fig. 5 we compare the light curves of SN 2006aj with those for SNe 1994I, 1998bw and 2002ap. Note that in this figure we have corrected the light curves for time dilation (for SNe 2006aj and 1998bw) and also corrected SN 2006aj for the underlying host galaxy. This correction is quite substantial, in particular at late stages (compare Fig. 1). The comparison in Fig. 5 demonstrates that SN 2006aj is in fact a fast version of SN 2002ap.

Another important aspect of GRB-SNe is clearly the possibility to relate the supernova shock-wave breakout with the exact time of the explosion. Campana et al. (2006) used the UVOT instrument onboard Swift to follow the UV lightcurves from the early shock break-out to the following peak due to radioactive heating (the latter being the optical peak we are probing in this paper). Such a shock break-out was also seen in SN 1999ex (Stritzinger et al. 2002) and in SN 1998bw (Galama et al. 1998). For SN 1999ex, the time of shock break-out could be estimated, and the rise time in the V band was $t(V) = 17.6$ days (Stritzinger et al. 2002). SN 2006aj has a substantially faster lightcurve, which is related to the faster expansion velocities, and possibly also to a lower ejecta mass.

4.2.3. X-ray Flash 060218

We note that GRB 060218 was a very soft burst, and thus qualifies as an (unusual) XRF. Campana et al. (2006) estimated $E_{\mathrm{peak}} = 4.9^{+0.4}_{-0.3}$ keV, at the very end of the observed distribution of peak energies. While the case for an association between long GRBs and SNe has been established (see Sect. 1), the case is more unclear for XRFs.

XRF 030723 showed a very conspicuous light curve bump at $\sim$16 days past burst, suggesting the presence of a fast rising supernova (Fynbo et al. 2004). In fact, doubts were raised against this interpretation since the required supernova light curve was very fast and narrow. The very fast U-band lightcurve of SN 2006aj may be taken as support for the hypothesis of a SN in XRF 030723. At a cosmological redshift of $\lesssim 1$ the R-band light curve bump would correspond to rest frame U, as also noted by Fynbo et al. (2004).

More recently, XRF 050824 showed a less conspicuous bump (Sollerman et al. 2006). Moreover, XRF 020903 has a lightcurve and spectrum consistent with a supernova at $z = 0.21$ (Soderberg et al. 2005; Bersier et al. 2006). These findings all argue for a common progenitor for GRBs and XRFs. The situation appeared less clear as other XRFs with late-time coverage did not show clear evidence for a bright supernova bump (e.g., Soderberg et al. 2005). However, with XRF 060218 the case for a supernova origin for such bursts is obvious.

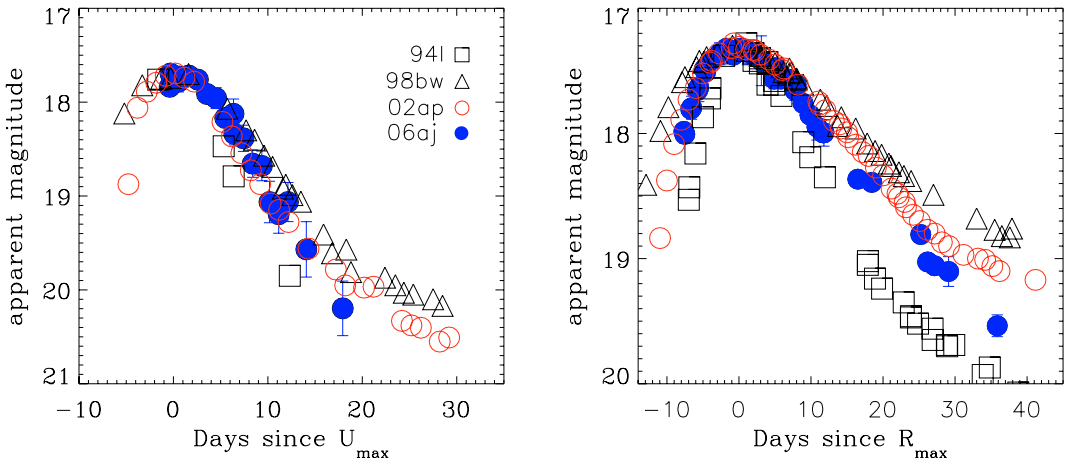

Fig. 5. Comparison of *U*- and *R*-band lightcurves for SN 2006aj and three other type Ic SNe. SN 1998bw is seen to evolve quite a bit slower, while SN 1994I is clearly faster. The best match is with SN 2002ap. The lightcurves have been corrected for time dilation and matched at date of peak and at maximum brightness. In this plot we have also corrected SN 2006aj for the host galaxy contribution. Note that the final *U*-band datapoint is uncertain due to a large relative host extinction correction.

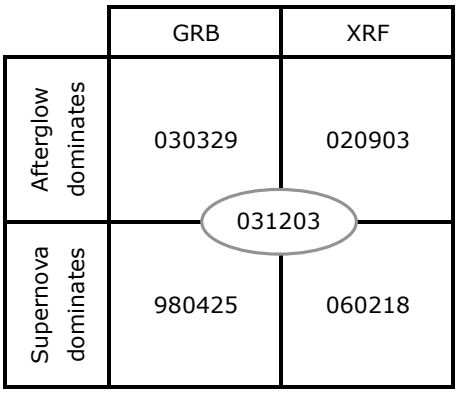

Fig. 6. Four-field diagram representing different varieties of Supernova-GRBs. There are differences in high-energy properties defining the peak energy of the burst, as well as in the optical afterglow appearance. XRF 060218/SN 2006aj fills in the lower right field of this diagram, as an XRF with supernova light dominating the early optical transient.

Among the many remaining questions are the lack of conspicuous afterglow emission. Compared to GRB 030329, the supernova emerged much faster from the afterglow for XRF 060218. It is interesting to note that there was also no conspicuous afterglow in SN 1998bw. For SN 2003lw (GRB 031203) there were claims of a very faint and fast decaying afterglow (Malesani et al. 2004). These bursts also had low values of $E_{\rm peak}$, and in fact Watson et al. (2004) considered 031203 to be an XRF. Ramirez-Ruiz et al. (2005) considered an off-axis model for XRF 031203 in which this was really a normal GRB although viewed from an angle of about twice the opening angle.

From Fig. 6 we see that it may be difficult to reconcile these diverse observations by a simple geometric scenario. In this four-field diagram we have divided bursts into XRFs and GRBs. We have also divided them according to the dominating component in the optical lightcurve; supernova or afterglow. We have indicated the spectroscopically confirmed SN-GRBs. The upper left corner is represented by GRB 030329 where SN 2003dh was not apparent until after a week. XRF 020903 was dominated by an afterglow until the late supernova bump, and occupies the upper right field. The same applies to XRF 030723. The lower left box is represented by SN 1998bw and GRB 980425, although the peak energy was not very high. Finally, XRF 060218 now fills in the lower right field in this diagram. It has a very low $E_{\rm peak}$ and shows supernova signatures already from the very early photometry (Campana et al. 2006) and spectroscopy (Modjaz et al. 2006; Mirabal et al. 2006, and this work Fig. 2).

A one-parameter explanation such as an on- vs. off-axis picture would have problem to explain all the combinations in Fig. 6. It seems that (SN)-XRFs can come both with and without a conspicious afterglow, and the afterglow can moreover behave quite differently (flat early lightcurve in XRF 030723 vs. constant decay in XRF 050824). A larger sample of SN-GRBs will be needed to unveil whether we observe different classes of objects, or simply a continuum of burst properties.

Thomsen et al. (2004) actually predicted Swift to detect a significant population of faint bursts and hence allow the study of core-collapse SNe at much earlier times than had been previously possible, and indicated that this would have a substantial impact on SN research. The discovery of the first nearby Swift GRB-SN substantiates this prediction.

Acknowledgements. This work was done at the Dark Cosmology Centre funded by The Danish National Research Foundation. JS also acknowledge support from Danmarks Nationalbank and from the Anna-Greta and Holger Crafoord fund. AOJ acknowledges support from the Norwegian Research Council. Some of the data presented here have been taken using ALFOSC, which is owned by the Instituto de Astrofisica de Andalucia (IAA) and operated at the Nordic Optical Telescope under agreement between IAA and the NBI.

References

Bersier, D., Fruchter, A. S., Strogler, L.-G., et al. 2006 [arXiv:astro-ph/0602163]
Bohlin, R. C., Colina, L., & Finley, D. S. 1995, AJ, 110, 1316
Bolzonella, M., Miralles, J.-M., & Pelló, R. 2000, A&A, 363, 476
Calzetti, D., Armus, L., Bohlin, R. C., et al. 2000, ApJ, 533, 682
Bertin, E., & Arnouts, S. 1996, A&AS, 117, 393
Campana, S., Mangano, V., Blusin, A. J., et al. 2006, Nature, submitted [arXiv:astro-ph/0603279]
Cool, R. J., Eisenstein, D. J., Hogg, D. W., et al. 2006, GCN, 4777
Cusumano, G., Barthelmy, S., Gehrels, N., et al. 2006, GCN, 4775
Fitzpatrick, E. L. 1986, AJ 92, 1068
Fukugita, M., Ichikawa, T., Gunn, J. E., Doi, M., Shimasaku, K., & Schneider, D. P. 1996, AJ, 111, 1748
Foley, R. J., Papenkova, M. S., Swift, B. J., et al. 2003, PASP, 115, 1220
Fynbo, J., Sollerman, J., Hjorth, J., et al. 2004, ApJ, 609, 962
Galama, T. J., Vreeswijk, P. M., van Paradijs, J., et al. 1998, Nature, 395, 670

Gal-Yam, A., Ofek, E. O., & Shemmer, O. 2002, MNRAS, 332, 73
Gehrels, N., Chincarini, G., Giommi, P., et al. 2004, ApJ, 611, 1005
Gorosabel, J., Perez-Ramirez, D., Sollerman, J., et al. 2005, A&A, 444, 711
Guenther, E. W., Klose, S., Vreeswijk, P., et al. 2006, GCN, 4863
Hicken, M., Modjaz, M., Challis, P., et al. 2006, GCN, 4898
Hjorth, J., Sollerman, J., Møller, P., et al. 2003, Nature, 423, 847
Höflich, P., Wheeler, J. C., & Wang, L. 1999, ApJ, 521, 179
Jakobsson, P., Levan, A., Fynbo, J. P. U., et al. 2006, A&A, 447, 897
Jester, S., Schneider, D. P., Richards, G. T., et al. 2005, AJ, 130, 873
Kennea, J. A., Burrows, D. N., Cusumano, G., et al. 2006, GCN, 4776
Kennicutt, R. C. 1998, ARA&A, 36, 189
Kewley, L. J., & Dopita, M. A. 2002, ApJS, 142, 35
Landolt, A. U. 1992, AJ, 104, 340
Malesani, D., Tagliaferri, G., Chincarini, G., et al. 2004, ApJ, 609, 5
Matheson, T., Garnavich, P. M., Stanek, K. Z., et al. 2003, ApJ, 599, 394
Masetti, N., Palazzi, E., Pian, E., et al. 2006, GCN, 4803
Mazzali, P. A., Deng, J., Maeda, K., et al. 2002, ApJ, 572, 61
Miller, G. E., & Scalo, J. M. 1979, ApJS, 41, 513
Mirabal, M., Halpern, J. P., et al. 2006, GCN, 4792
Mirabal, M., Halpern, J. P., An, D., Thorstensen, J. R., & Terndrup, D. M. 2006 [arXiv:astro-ph/0603686]
Modjaz, M., Stanek, K. Z., Garnavich, P. M., et al. 2006 [arXiv:astro-ph/0603377]
Munari, U., & Zwitter, T. 1997, A&A, 318, 269
Pandey, S. B., Anupama, G. C., Sagar, R., Bhattacharya, D., Sahu, D. K., & Pandey, J. C. 2003, MNRAS, 340, 375
Patat, F., Cappellaro, E., Danziger, J., et al. 2001, ApJ, 555, 900
Pei, Y. C. 1992, ApJ, 395, 130
Pian, E., Mazzali, P., Masetti, N., et al. 2006 [arXiv:astro-ph/0603530]
Prevot, M. L., Lequeux, J., Prevot, L., Maurice, E., & Rocca-Volmerange, B. 1984, A&A, 132, 389
Ramirez-Ruiz, E., Granot, J., Kouveliotou, C., et al. 2005, ApJ, 625, L91
Richardson, D., Branch, D., & Baron, E. 2006 [arXiv:astro-ph/0601136]
Richmond, M. W., van Dyk, S. D., Ho, W., et al. 1996, AJ, 111, 327
Salpeter, E. E. 1955, ApJ, 121, 161
Scalo, J. M. 1986, Fund. Cosmic Phys., 11, 1
Schlegel, D. J., Finkbeiner, D. P., & Davis, M. 1998, ApJ, 500, 525
Seaton, M. J. 1979, MNRAS, 187, 73
Soderberg, A. M., Kulkarni, S. R., Fox, D. B., et al. 2005, ApJ, 627, 877
Soderberg, A. M., Frail, D., et al. 2006, GCN, 4794
Soderberg, A., Berger, E., & Schmidt, B. 2006, IAUC, 8674
Sollerman, J., Kozma, C., Fransson, C., et al. 2000, ApJ, 537, L127
Sollerman, J., Cox, N., Mattila, S., et al. 2005a, A&A, 429, 559
Sollerman, J., Östlin, G., Fynbo, J. P. U., et al. 2005b, New Astron., 11, 103
Sollerman, J., Fynbo, J. P. U., et al. 2006, in preparation
Stanek, K. Z., Matheson, T., Garnavich, P. M., et al. 2003, ApJ, 591, L17
Stetson, P. B. 1987, PASP, 99, 191
Stritzinger, M., Hamuy, M., Suntzeff, N. B., et al. 2002, AJ, 124, 2100
Stritzinger, M., Leibundgut, B., Walch, S., & Contardo, G. 2006, A&A, in press [arXiv:astro-ph/0506415]
Thomsen, B., Hjorth, J., Watson, D., et al. 2004, A&A, 419, 21
Watson, D., Hjorth, J., Levan, A., et al. 2004, ApJ, 605, 101
Woosley, S. E., Eastman, R. G., & Schmidt, B. P. 1999, ApJ, 516, 788

Online Material

Table 4. Log of observations and photometry of supernova 2006aj.

Date (UT)	Δt (days)	Pass band	Exptime (s)	Magnitude	Magnitude Error (1σ)	Telescope
Feb. 23.932	5.783	*U*	900	17.74	0.06	NOT
Feb. 24.006	5.857	*U*	120	17.43	0.30	D1.5 m
Feb. 24.009	5.860	*U*	200	17.33	0.16	D1.5 m
Feb. 24.012	5.863	*U*	200	17.55	0.07	D1.5 m
Feb. 24.016	5.867	*U*	200	17.61	0.06	D1.5 m
Feb. 24.022	5.873	*U*	600	17.66	0.04	D1.5 m
Feb. 24.030	5.881	*U*	600	17.60	0.04	D1.5 m
Feb. 24.898	6.749	*U*	300	17.69	0.10	NOT
Feb. 25.009	6.860	*U*	200	17.62	0.09	D1.5 m
Feb. 25.014	6.865	*U*	400	17.67	0.06	D1.5 m
Feb. 25.021	6.872	*U*	600	17.64	0.04	D1.5 m
Feb. 25.029	6.880	*U*	600	17.63	0.05	D1.5 m
Feb. 26.006	7.857	*U*	200	17.65	0.24	D1.5 m
Feb. 26.011	7.862	*U*	200	17.51	0.12	D1.5 m
Feb. 26.016	7.867	*U*	600	17.66	0.03	D1.5 m
Feb. 26.024	7.875	*U*	600	17.71	0.03	D1.5 m
Feb. 27.008	8.859	*U*	200	17.35	0.17	D1.5 m
Feb. 27.011	8.862	*U*	200	17.61	0.10	D1.5 m
Feb. 27.017	8.868	*U*	600	17.69	0.05	D1.5 m
Feb. 27.025	8.876	*U*	600	17.72	0.05	D1.5 m
Feb. 28.007	9.858	*U*	200	17.57	0.16	D1.5 m
Feb. 28.010	9.861	*U*	200	17.79	0.10	D1.5 m
Feb. 28.016	9.867	*U*	600	17.77	0.08	D1.5 m
Feb. 28.024	9.875	*U*	600	17.87	0.04	D1.5 m
Mar. 1.012	10.863	*U*	600	17.85	0.10	D1.5 m
Mar. 2.003	11.854	*U*	200	18.48	0.24	D1.5 m
Mar. 2.007	11.858	*U*	200	18.16	0.25	D1.5 m
Mar. 2.012	11.863	*U*	600	18.04	0.08	D1.5 m
Mar. 2.914	12.765	*U*	300	18.00	0.14	NOT
Mar. 3.003	12.854	*U*	200	18.06	0.18	D1.5 m
Mar. 3.009	12.860	*U*	600	18.19	0.10	D1.5 m
Mar. 4.005	13.856	*U*	200	18.01	0.15	D1.5 m
Mar. 4.010	13.861	*U*	600	18.45	0.08	D1.5 m
Mar. 5.005	14.856	*U*	200	18.31	0.18	D1.5 m
Mar. 5.011	14.862	*U*	600	18.46	0.12	D1.5 m
Mar. 6.006	15.857	*U*	200	18.57	0.20	D1.5 m
Mar. 6.012	15.863	*U*	600	18.48	0.13	D1.5 m
Mar. 6.851	16.702	*U*	900	18.79	0.17	NOT
Mar. 7.854	17.705	*U*	900	18.89	0.15	NOT
Mar. 8.866	18.717	*U*	900	18.79	0.16	NOT
Mar. 10.878	20.729	*U*	1500	19.16	0.20	NOT
Mar. 14.864	24.715	*U*	2400	19.55	0.15	NOT
Feb. 21.013	2.864	*V*	120	18.22	0.05	D1.5 m
Feb. 21.015	2.866	*V*	120	18.16	0.08	D1.5 m
Feb. 21.017	2.868	*V*	120	18.21	0.03	D1.5 m
Feb. 21.034	2.885	*V*	300	18.21	0.03	D1.5 m
Feb. 21.051	2.902	*V*	600	18.17	0.03	D1.5 m
Feb. 22.020	3.871	*V*	120	18.01	0.03	D1.5 m
Feb. 22.022	3.873	*V*	120	18.02	0.05	D1.5 m
Feb. 22.040	3.891	*V*	300	18.01	0.03	D1.5 m
Feb. 22.045	3.896	*V*	300	18.00	0.03	D1.5 m
Feb. 22.049	3.900	*V*	300	18.03	0.03	D1.5 m
Feb. 23.027	4.878	*V*	300	17.84	0.05	D1.5 m
Feb. 23.031	4.882	*V*	300	17.87	0.02	D1.5 m
Feb. 23.046	4.897	*V*	300	17.84	0.03	D1.5 m
Feb. 23.050	4.901	*V*	300	17.85	0.04	D1.5 m
Feb. 24.041	5.892	*V*	300	17.71	0.04	D1.5 m
Feb. 25.041	6.892	*V*	300	17.61	0.03	D1.5 m
Feb. 26.031	7.882	*V*	300	17.53	0.03	D1.5 m
Feb. 27.032	8.883	*V*	300	17.50	0.04	D1.5 m
Feb. 28.031	9.882	*V*	300	17.49	0.04	D1.5 m
Mar. 1.018	10.869	*V*	200	17.50	0.08	D1.5 m
Mar. 2.019	11.870	*V*	200	17.50	0.03	D1.5 m

Table 1. continued.

Date (UT)	Δt (days)	Pass band	Exptime (s)	Magnitude	Magnitude Error (1σ)	Telescope
Mar. 2.924	12.775	*V*	300	17.52	0.04	NOT
Mar. 3.016	12.867	*V*	200	17.54	0.05	D1.5 m
Mar. 4.017	13.868	*V*	200	17.61	0.03	D1.5 m
Mar. 5.018	14.869	*V*	200	17.62	0.15	D1.5 m
Mar. 6.863	16.714	*V*	300	17.77	0.10	NOT
Mar. 7.002	16.853	*V*	300	17.74	0.04	D1.5 m
Mar. 7.012	16.863	*V*	300	17.81	0.02	D1.5 m
Mar. 7.863	17.714	*V*	300	17.85	0.08	NOT
Mar. 8.002	17.853	*V*	300	17.92	0.07	D1.5 m
Mar. 8.006	17.857	*V*	300	17.84	0.07	D1.5 m
Mar. 8.874	18.725	*V*	300	18.00	0.09	NOT
Mar. 9.008	18.859	*V*	450	17.94	0.04	D1.5 m
Mar. 9.837	19.688	*V*	300	18.04	0.11	NOT
Mar. 11.004	20.855	*V*	300	18.12	0.07	D1.5 m
Mar. 12.000	21.851	*V*	200	18.20	0.07	D1.5 m
Mar. 12.999	22.850	*V*	100	18.24	0.17	D1.5 m
Mar. 13.859	23.710	*V*	900	18.26	0.06	NOT
Mar. 13.995	23.846	*V*	100	18.29	0.09	D1.5 m
Mar. 15.992	25.843	*V*	180	18.34	0.12	D1.5 m
Mar. 18.840	28.691	*V*	900	18.65	0.07	NOT
Mar. 20.852	30.703	*V*	900	18.78	0.06	NOT
Feb. 21.021	2.872	*R*	200	18.00	0.02	D1.5 m
Feb. 21.025	2.876	*R*	300	17.97	0.09	D1.5 m
Feb. 21.029	2.880	*R*	300	17.99	0.09	D1.5 m
Feb. 21.041	2.892	*R*	600	17.99	0.07	D1.5 m
Feb. 21.057	2.908	*R*	150	18.00	0.08	D1.5 m
Feb. 21.915	3.766	*R*	900	17.79	0.03	NOT
Feb. 22.026	3.877	*R*	300	17.80	0.04	D1.5 m
Feb. 22.031	3.882	*R*	300	17.82	0.06	D1.5 m
Feb. 22.054	3.905	*R*	300	17.81	0.08	D1.5 m
Feb. 22.898	4.749	*R*	900	17.64	0.03	NOT
Feb. 23.016	4.867	*R*	200	17.62	0.07	D1.5 m
Feb. 23.019	4.870	*R*	200	17.64	0.08	D1.5 m
Feb. 23.023	4.874	*R*	200	17.63	0.09	D1.5 m
Feb. 23.036	4.887	*R*	300	17.61	0.08	D1.5 m
Feb. 23.041	4.892	*R*	300	17.64	0.09	D1.5 m
Feb. 23.879	5.730	*R*	250	17.51	0.04	NOT
Feb. 24.036	5.887	*R*	300	17.49	0.10	D1.5 m
Feb. 24.854	6.705	*R*	300	17.36	0.04	NOT
Feb. 25.036	6.887	*R*	300	17.38	0.05	D1.5 m
Feb. 26.036	7.887	*R*	300	17.29	0.03	D1.5 m
Feb. 27.037	8.888	*R*	300	17.25	0.08	D1.5 m
Feb. 28.035	9.886	*R*	300	17.21	0.02	D1.5 m
Mar. 1.023	10.874	*R*	200	17.26	0.04	D1.5 m
Mar. 2.022	11.873	*R*	200	17.21	0.03	D1.5 m
Mar. 2.849	12.700	*R*	300	17.22	0.03	NOT
Mar. 3.020	12.871	*R*	200	17.24	0.09	D1.5 m
Mar. 4.020	13.871	*R*	200	17.26	0.08	D1.5 m
Mar. 5.022	14.873	*R*	200	17.30	0.18	D1.5 m
Mar. 6.843	16.694	*R*	300	17.43	0.07	NOT
Mar. 7.016	16.867	*R*	300	17.34	0.06	D1.5 m
Mar. 7.020	16.871	*R*	200	17.35	0.03	D1.5 m
Mar. 7.867	17.718	*R*	300	17.43	0.06	NOT
Mar. 8.012	17.863	*R*	300	17.40	0.02	D1.5 m
Mar. 8.017	17.868	*R*	300	17.43	0.05	D1.5 m
Mar. 8.848	18.699	*R*	1500	17.43	0.03	NOT
Mar. 9.841	19.692	*R*	300	17.51	0.07	NOT
Mar. 10.010	19.861	*R*	400	17.47	0.07	D1.5 m
Mar. 11.009	20.860	*R*	300	17.60	0.03	D1.5 m
Mar. 12.005	21.856	*R*	400	17.68	0.02	D1.5 m
Mar. 13.001	22.852	*R*	150	17.76	0.09	D1.5 m
Mar. 13.872	23.723	*R*	900	17.80	0.04	NOT

Table 1. continued.

Date (UT)	Δt (days)	Pass band	Exptime (s)	Magnitude	Magnitude Error (1σ)	Telescope
Mar. 13.998	23.849	*R*	100	17.79	0.08	D1.5 m
Mar. 14.000	23.851	*R*	100	17.81	0.06	D1.5 m
Mar. 18.860	28.711	*R*	900	18.10	0.04	NOT
Mar. 20.866	30.717	*R*	900	18.12	0.04	NOT
Mar. 27.889	37.740	*R*	1800	18.43	0.04	NOT
Mar. 28.874	38.725	*R*	1800	18.58	0.03	NOT
Mar. 29.874	39.725	*R*	2100	18.60	0.03	NOT
Mar. 31.884	41.735	*R*	1800	18.63	0.08	NOT
Apr. 07.858	48.709	*R*	1800	18.89	0.05	NOT